Sea level changes forced by Southern Ocean winds

Leela M. Frankcombe,[1,2] Paul Spence,[1,2] Andrew McC. Hogg,[1,3] Matthew H. England,[1,2] and Stephen M. Griffies[1,4]

Received 25 September 2013; accepted 11 October 2013; published 5 November 2013.

[1] On regional scales, changes in sea level are significantly affected by local dynamical changes. Westerly winds over the Southern Ocean have been strengthening and shifting southward in recent decades, and this change is projected to continue in the future. This study applies wind forcing anomalies to an eddy-permitting ocean model to study the dynamical response to a Southern Hemisphere westerly wind increase and/or southward shift. It is shown that the applied wind anomalies result in a change in sea surface slope across the Antarctic Circumpolar Current such that a fall in sea level occurs around the Antarctic continental margin. The Antarctic Circumpolar Current transport and regional sea level are particularly sensitive to latitudinal shifts in the wind, with a much more muted response found when only wind strengthening is applied. In addition to the local sea level changes, Southern Ocean winds also have a global effect through changing ocean heat content and the global overturning circulation. **Citation:** Frankcombe, L. M., P. Spence, A. McC. Hogg, M. H. England, and S. M. Griffies (2013), Sea level changes forced by Southern Ocean winds, *Geophys. Res. Lett.*, *40*, 5710–5715, doi:10.1002/2013GL058104.

1. Introduction

[2] Global mean sea level (GMSL) changes are often studied in terms of balancing the net sea level budget [*Gregory et al.*, 2013]. Regional sea level changes can, however, differ considerably from the global mean; in order to explain the spatial patterns of sea level change, we must also take dynamical effects (due to local changes in temperature, salinity, and ocean circulation) and static effects (due to mass redistribution) into account [*Slangen et al.*, 2012]. Regional processes are important in the tropical Pacific, for example, where strengthening of the trade winds has caused sea level rise in the west and fall in the east relative to the global mean over the past two decades [*McGregor et al.*, 2012].

[3] In the Southern Ocean, observations reveal a poleward intensification of the westerly winds since the 1950s. This intensification corresponds to a positive shift in the Southern Annular Mode (SAM) and has been attributed to increasing atmospheric concentrations of ozone-depleting and greenhouse gases [*Thompson et al.*, 2011]. Global climate models are remarkably consistent in simulating a continuation of the observed positive SAM trend through the 21st century [*Meijers et al.*, 2012], yet sea level changes in this region have received little attention.

[4] The SAM trend can impact local and global sea level by changing the pattern and magnitude of wind stress, and by modifying surface buoyancy fluxes [*Sen Gupta and England*, 2006], which may in turn alter the strength and/or position of the Antarctic Circumpolar Current (ACC) [*Spence et al.*, 2010; *Shakespeare and Hogg*, 2012], the intensity of the eddy field [*Meredith and Hogg*, 2006], and the strength of the meridional overturning circulation [*Sijp and England*, 2009]. Our ability to accurately predict regional sea level changes in the Southern Ocean as well as the rate of global mean sea level change due to thermal expansion may thus depend on a better understanding of the Southern Ocean winds and circulation. The complex interplay between eddies and the large scale circulation [e.g., *Morrison and Hogg*, 2013] motivates the use of eddy-permitting models to study this problem.

[5] Observations of sea level around Antarctica prior to the satellite era are sparse and even now the presence of sea ice complicates satellite measurements close to the continent. For this reason, many studies of the Southern Ocean rely on model results. *Bouttes et al.* [2012] found a dipole-like structure in sea level change in Coupled Model Intercomparison Project (CMIP) phase 3 SRESA1B and phase 5 1%CO_2 runs, with sea level rising north of 50°S and falling to the south in the multimodel mean. They linked this pattern to changes in Southern Ocean winds, with the caveat that CMIP models do not have sufficient resolution to explicitly resolve mesoscale eddies. In this study, we use a global eddy-permitting ocean model to investigate the dynamical effect of idealized wind changes over the Southern Ocean on regional and global sea level.

2. The Model

[6] This study uses the Australian Community Climate and Earth System Simulator - Ocean-Eddy Permitting (ACCESS-OEP) global ocean-sea ice model, which is based on the Geophysical Fluid Dynamics Laboratory CM2.4 and CM2.5 fully coupled climate models [*Farneti et al.*, 2010; *Delworth et al.*, 2012]. The model has a 1/4° horizontal resolution with a bipolar Arctic north of 65°N, and a Mercator grid south to 65°S (∼11 km grid spacing at 65°S). The model has 50 vertical levels and is coupled to the Geophysical Fluid Dynamics Laboratory (GFDL) Sea Ice Simulator dynamic/thermodynamic sea ice model.

Additional supporting information may be found in the online version of this article.

[1]ARC Centre of Excellence for Climate System Science.
[2]Climate Change Research Centre, University of New South Wales, Sydney, New South Wales, Australia.
[3]Research School of Earth Sciences, Australian National University, Canberra, ACT, Australia.
[4]NOAA Geophysical Fluid Dynamics Laboratory, Princeton, New Jersey, USA.

Corresponding author: L. Frankcombe, Climate Change Research Center, Level 4 Mathews Bldg., University of New South Wales, Sydney, NSW 2052, Australia. (l.frankcombe@unsw.edu.au)

0094-8276/13/10.1002/2013GL058104

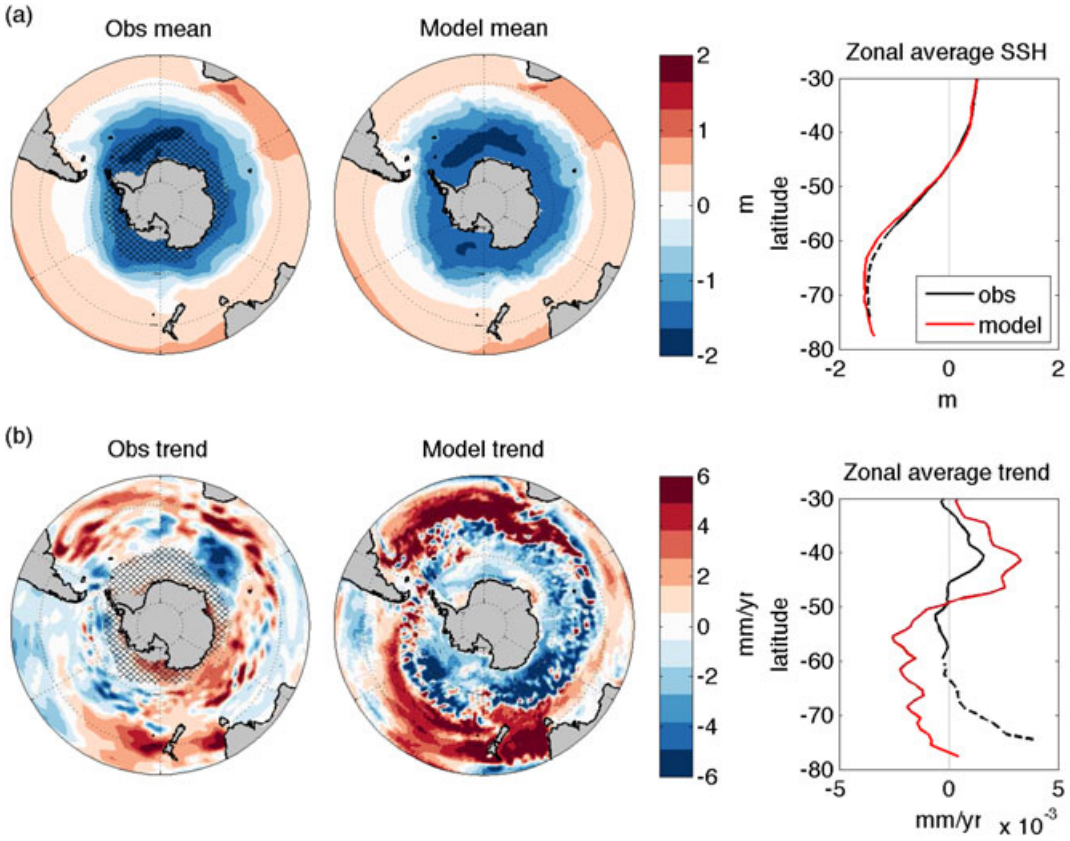

Figure 1. Observed and modeled sea level (a) mean (in m) and (b) trend (in mm/yr) over the period 1993–2007, shown in both latitude-longitude coordinates and as a zonal mean. For the altimetry, the hatching indicates regions in which the observations may be influenced by sea ice.

[7] The simulations are all forced at the surface with 6-hourly Coordinated Ocean-Ice Reference Experiments (CORE) version 2 reanalysis data sets that include synoptic variability [*Large and Yeager*, 2009]. The atmospheric state is prescribed and ocean surface fluxes are determined by bulk formulae.

[8] In the first experiment, an interannually forced (IAF) simulation is integrated through six cycles of 1948–2007 forcing from the CORE-IAF_v2 data. In order to assess the accuracy of the model in simulating observed sea level variability, the last forcing cycle is compared to satellite observations.

[9] A second set of simulations is used to assess the impact of changing Southern Ocean winds on sea level. A control simulation is equilibrated with a repeating climatological "normal" year of atmospheric forcing (NYF) [*Griffies et al.*, 2009] derived from the CORE-NYF_v2 data. Three perturbed Southern Ocean wind forcing experiments are then initiated from year 100 of the NYF run. The perturbed NYF wind is applied between 25°S and 70°S with sinusoidal smoothing within 5° of the forcing boundaries. Both zonal and meridional components of the wind are altered to prevent unrealistic decompositions of the synoptic variability. In the $W_{4°S}$, $W_{+15\%}$, and $W_{4°S+15\%}$ simulations, the NYF 10 m winds are shifted 4°S, increased in speed by 15% (with wind stress computed by the bulk formulae), and poleward intensified by 4° and 15%, respectively. The wind forcing perturbations are applied instantaneously and then held constant for 70 years (after which time, while the models are not in thermodynamic equilibrium, the trends in the fields investigated here have been consistent for decades). The latitude shift and magnitude change were chosen to be at the upper end of the range simulated for the end of the 21st century by CMIP3 [*Fyfe et al.*, 2007] and CMIP5 models [*Bouttes et al.*, 2012]; therefore, our results represent an upper bound on projected changes caused by changing Southern Ocean winds. While we use a prescribed atmospheric state in this study, future work should examine the robustness of the results with a coupled model as air-sea feedbacks can alter how and where heat accumulates in the ocean.

[10] Sea level is an integral of the whole of the ocean and is thus sensitive to deep ocean drift from incomplete equilibration. The drift was estimated in the IAF simulation by using the linear trend over the last three forcing cycles and in the perturbed NYF experiments by using the NYF control run (which was also integrated for another 70 years).

[11] All experiments here explicitly include the effects of permitted eddies; we do not attempt quantitative comparison with coarse resolution models, as any such comparison is controlled by choices relating to eddy parameterization at coarse resolution.

3. Observed and Modeled 1993–2007 Trends

[12] We start by comparing the last forcing cycle of the IAF simulation with a blended satellite altimetry product supplied by the Physical Oceanography Distributed Active

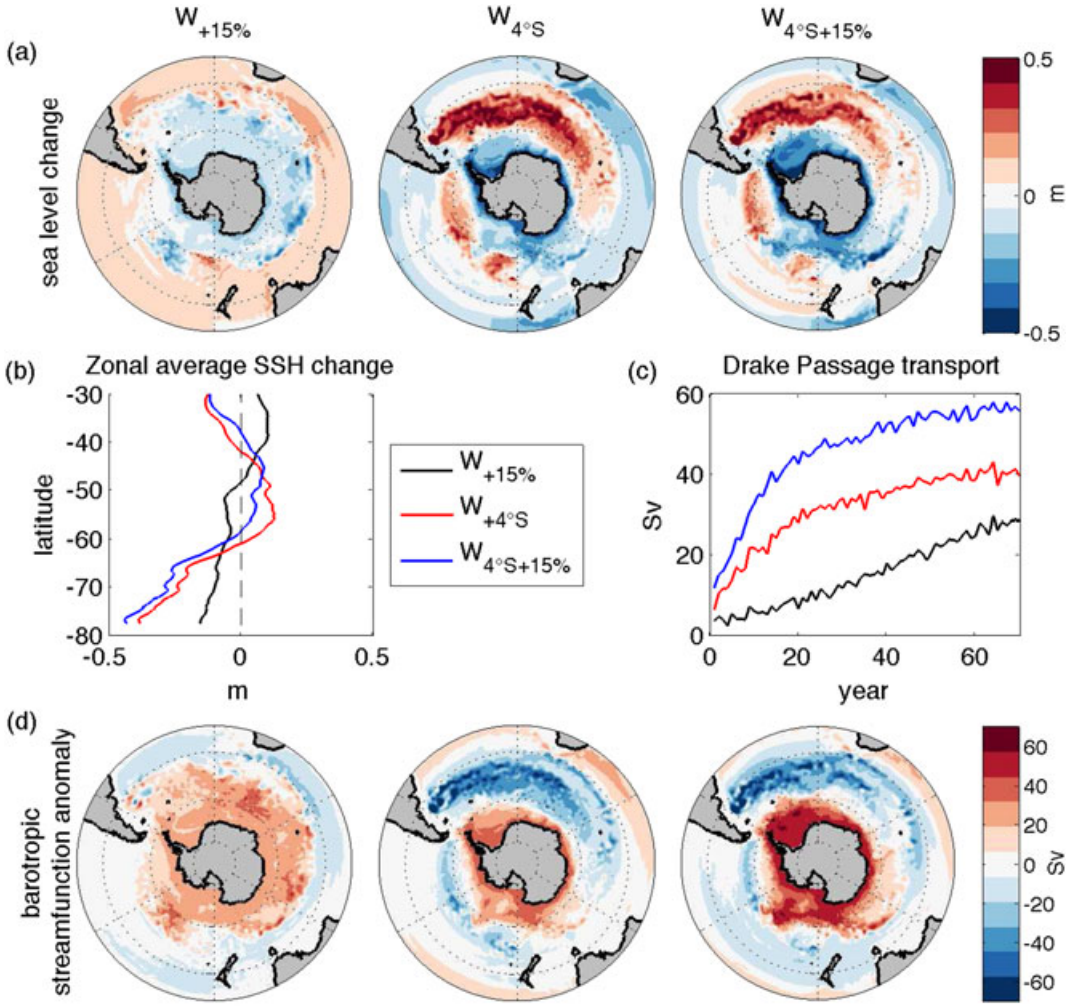

Figure 2. (a) Sea level change (in m), (b) zonally averaged sea level change (in m), (c) Drake Passage transport anomalies (in Sv; 1 Sv = 10^6 m^3/s), and (d) barotropic stream function anomalies (in Sv) in the three perturbed NYF runs, relative to the control. The results in Figures 2a, 2b, 2d, and in the subsequent figures are averaged over the last 10 years of the run and have the corresponding period from the control run subtracted.

Archive Center at the NASA Jet Propulsion Laboratory (http://podaac.jpl.nasa.gov/dataset/AVISO_L4_DYN_TOPO_1DEG_1MO). The observed and modeled sea level mean and linear trend over the period 1993–2007 (over which both model and observations are available) are plotted in Figure 1. No observations are plotted south of 75°S, and regions affected by winter sea ice are hatched to indicate decreased reliability of the observations. The GMSL rise of *Church and White* [2011] has been removed from each grid point of the altimetry so that it is comparable to the model (which uses the Boussinesq formulation and thus does not simulate GMSL directly). The modeled mean agrees well with observations. The observed and modeled trends have a qualitatively similar pattern, with sea level rising faster than the global mean north of 50°S and more slowly between 50° and 60°S; however, there is disagreement on the sign of the change south of 60° (where observations are not reliable). The modeled trends are also larger and more zonally symmetric than observed trends, which may be due to a spurious post-1979 trend in the NCEP-based CORE winds [*Brodeau et al.*, 2010]. Note that this spurious wind forcing trend does not apply to the idealized simulations in the next section.

4. Sea Level Response to Perturbed NYF Winds

[13] Next, we turn to the three runs forced by perturbed NYF Southern Ocean wind anomalies. Figure 2a shows sea level change in the Southern Ocean in each run relative to the NYF control (for sea level change in other oceans, see Figure S1 in the supporting information). The $W_{+15\%}$ run shows a sea level rise over most of the global ocean north of 50°S and a fall to the south, which in the Southern Ocean resembles the pattern of sea level change in CMIP3+5 models [*Bouttes et al.*, 2012]. Both $W_{4°S}$ and $W_{4°S+15\%}$ show a decrease in sea level over most of the global ocean. Large changes are restricted to the Southern Ocean where there are large areas of sea level rise around 40–60°S and sea level fall around the coast of Antarctica. There is a drop of about 0.4 m very close to Antarctica in the zonal mean in these two runs and a smaller fall of about 0.15 m in $W_{+15\%}$, as shown in Figure 2b.

[14] Figure 2c shows that for all three perturbed NYF experiments there is an increase in Drake Passage transport. For $W_{+15\%}$, this transport increase is simply an adjustment of the geostrophic balance—increased winds move light water northwards, gradually deepening the pycnocline to the north,

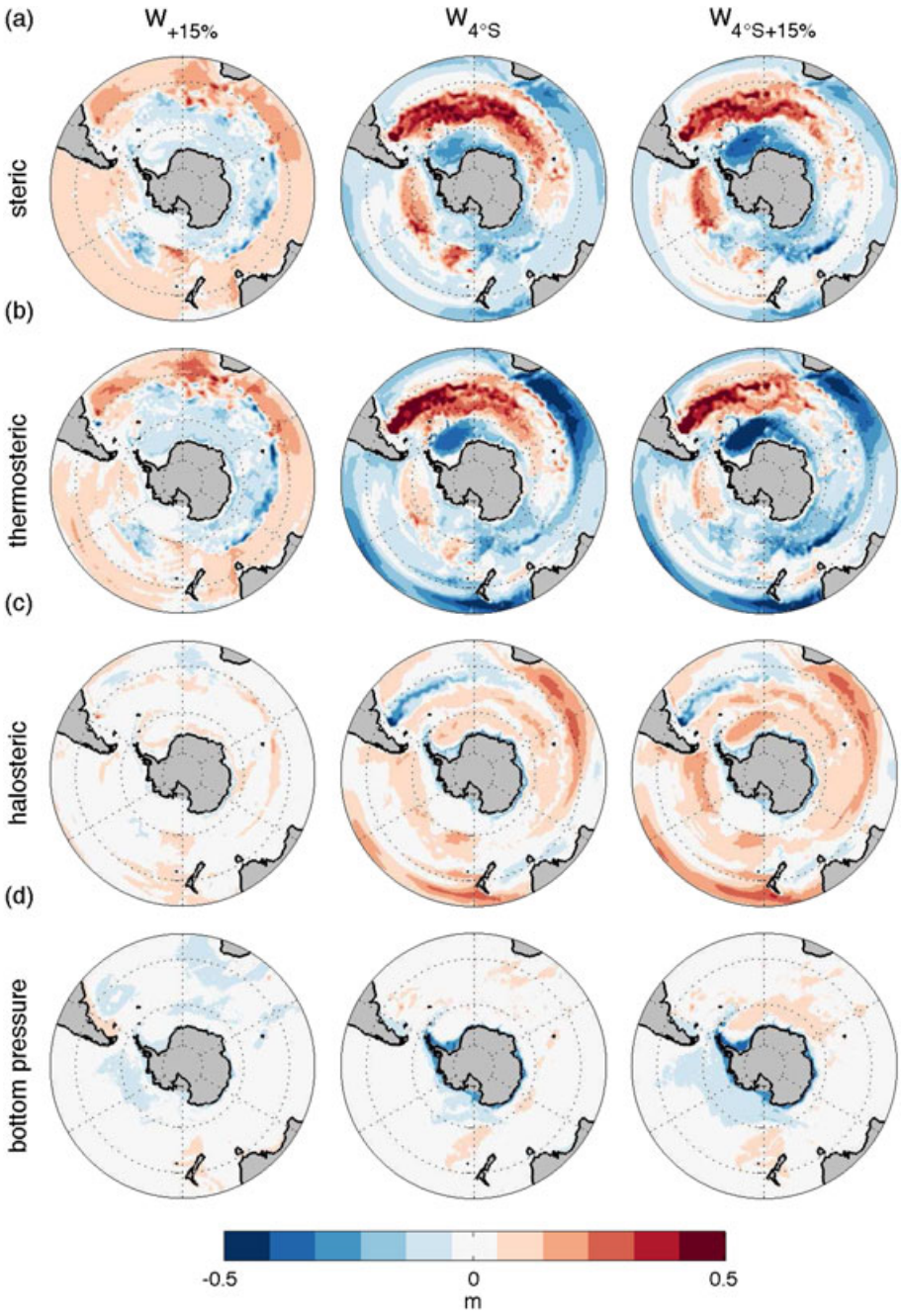

Figure 3. Sea level change (in m) in the three perturbed NYF runs decomposed into components as follows: (a) the steric component, in turn decomposed into (b) thermosteric and (c) halosteric parts, and (d) the bottom pressure component.

and building up an increased sea level gradient over the ACC (the black line in Figure 2b), leading to a gradual increase in current strength. For $W_{4°S}$, ACC transport increases more rapidly, also due to steepening of the meridional sea level gradient over the ACC (red line in Figure 2b). North of the ACC, the wind shift causes temperature fronts to shift southward, particularly in the Atlantic sector [*Spence et al.*, 2010], which increases heat loss from the ocean. South of the ACC, a large ice-free area develops in the Weddell Sea in the first decade of the simulation, in a similar position to the Weddell Polynya observed in the 1970s [*Carsey*, 1980]. The model polynya persists for about three winter seasons and leads to a deepening of the mixed layer which remains throughout the rest of the simulation. Associated with this deeper mixing is an increase in Antarctic Bottom Water (AABW) formation, greater cross-ACC density gradients, and a lowering of sea level in the Weddell Sea. The combination of southward shifted temperature fronts north of the ACC and density change to the south leads to a much steeper sea level gradient across the ACC in $W_{4°S}$ and thus to an increase in Drake Passage transport, in line with *Shakespeare and Hogg* [2012] who found that ACC transport scales with the formation rate of AABW. Figure 2d shows barotropic stream function anomalies for the three runs; there is a strong inverse correlation between these anomalies and the sea level change in Figure 2a.

[15] The steric component of the sea level change, due to density changes in the water column, is plotted in Figure 3

for the three perturbed NYF runs. This steric component can be partitioned into the thermosteric component, due to temperature changes, and the halosteric component, due to salinity changes. These components are also plotted in Figure 3, along with the bottom pressure component, which is due to the movement of mass from one part of the ocean to another. This movement of mass can be caused by circulation changes or by changes in global ocean volume causing water to move between the shelves and the deep ocean [*Landerer et al.*, 2007].

[16] The largest component of sea level change induced in the Southern Ocean by the perturbed NYF winds is due to temperature changes in response to the shifting winds. Temperature changes are offset in some places by salinity changes (i.e., the thermosteric and halosteric components partially compensate each other) [*Lowe and Gregory*, 2006], such as in the Agulhas retroflection and to a lesser extent in the Atlantic sector of the Southern Ocean (as well as almost perfect compensation over much of the North Atlantic; see Figure S1). There is partial compensation over the Antarctic shelf region such that the overall steric contribution is small. Further off the shelf, however, density changes in the Weddell Sea and the southward shift of temperature fronts both contribute to the thermosteric component, causing large changes in sea level.

[17] Each of the three perturbed NYF runs shows a change in global ocean heat content of approximately 2% compared to the control, with $W_{+15\%}$ warming and both $W_{4°S}$ and $W_{4°S+15\%}$ cooling. In both $W_{4°S}$ and $W_{4°S+15\%}$, there are large heat losses from the Southern Ocean due to the southward shifted temperature fronts. In contrast, $W_{+15\%}$ shows increasing ocean heat content in the Southern Ocean. These changes in global ocean heat content imply that there will be changes in GMSL. We follow *Griffies and Greatbatch* [2012, see equation 225] to compute GMSL in our Boussinesq ocean model and find an increase of approximately 0.04 m in $W_{+15\%}$ and decreases of approximately 0.06 m in $W_{4°S}$ and 0.05 m in $W_{4°S+15\%}$ over the 70 years of the simulation. For comparison, *Church and White* [2011] calculated $\sim$ 3 mm/yr rise in sea level over 1993–2009, yielding a 0.21 m increase over 70 years.

[18] In $W_{4°S}$ and $W_{4°S+15\%}$, the bottom pressure term is positive over the deep ocean and negative over the shelves, indicating that water is moving off the shelves as expected for a decline in GMSL. In $W_{+15\%}$, the bottom pressure term is positive on the shelves due to the rise in GMSL (except on the Antarctic shelf). The bottom pressure term is negative on the Antarctic shelf, and there is a decrease in sea level along the coastline of Antarctica in all three runs, despite the fact that one has a rise and the other two a fall in GMSL. This decrease in bottom pressure and fall in sea level are due to movement of water off the Antarctic shelf due to the change in sea level gradient across the ACC, rather than due to changes in global ocean volume (which explains the sea level changes on other shelves).

5. Conclusions

[19] In terms of regional sea level changes, we find that the thermosteric effect is largely responsible for the patterns of sea level change due to changing winds in the Southern Ocean. These patterns agree with those simulated by CMIP3+5 models, as discussed by *Bouttes et al.* [2012], indicating that the qualitative regional sea level response does not appear to be sensitive to eddies. Sea level changes are accompanied by changes in ACC strength and closely mirror changes in barotropic stream function. Increasing wind stress directly drives an increase in ACC strength while shifting the winds has a more immediate and dramatic impact by shifting temperature fronts north of the ACC southward and by decreasing density to the south (particularly due to mixed layer deepening in the Weddell Sea).

[20] One striking effect of the altered density gradient across the ACC is the drop in sea level along the Antarctic coast in all three perturbed NYF runs. This fall would partially offset GMSL rise in the region and should be taken into account when considering ice sheet stability [*Gomez et al.*, 2010]. This sea level fall is particularly sensitive to the southward shift in Southern Ocean winds.

[21] The change of global ocean heat content and thus GMSL in the three runs illustrates the important role of Southern Ocean winds in controlling the uptake and redistribution of heat throughout the global ocean. We show that increasing the Southern Ocean wind stress increases heat uptake, thus raising GMSL, while shifting the winds poleward causes heat uptake to decrease, lowering GMSL.

[22] **Acknowledgments.** We thank W. Anderson, T. Delworth, and M. Winton at GFDL for support during this project, H.-C. Lee and W. Anderson for help running the interannual CORE simulation, and M. Ward for help running the perturbed NYF simulations. This work was supported by the Australian Research Council, including the ARC Centre of Excellence for Climate System Science, and an award under the Merit Allocation Scheme on the NCI National Facility at the ANU.

[23] The Editor thanks two anonymous reviewers for their assistance in evaluating this paper.

References

Bouttes, N., J. M. Gregory, T. Kuhlbrodt, and T. Suzuki (2012), The effect of windstress change on future sea level change in the Southern Ocean, *Geophys. Res. Lett.*, *39*, L23602, doi:10.1029/2012GL054207.

Brodeau, L., B. Barnier, A.-M. Treguier, T. Penduff, and S. Gulev (2010), An ERA40-based atmospheric forcing for global ocean circulation models, *Ocean Modell.*, *31*(3-4), 88–104, doi:10.1016/j.ocemod.2009.10.005.

Carsey, F. D. (1980), Microwave Observation of the Weddell Polynya, *Mon. Wea. Rev.*, *108* (12), 2032–2044, doi:10.1175/1520-0493(1980)108<2032:MOOTWP>2.0.CO;2.

Church, J. A., and N. J. White (2011), Sea-level rise from the Late 19th to the Early 21st Century, *Surv. Geophys.*, *32* (4-5), 585–602, doi:10.1007/s10712-011-9119-1.

Delworth, T. L., et al. (2012), Simulated climate and climate change in the GFDL CM2.5 high-resolution coupled climate model, *J. Clim.*, *25*, 2755–2781, doi:10.1175/JCLI-D-11-00316.

Farneti, R., T. L. Delworth, A. J. Rosati, S. M. Griffies, and F. Zeng (2010), The role of mesoscale eddies in the rectification of the Southern Ocean response to climate change, *J. Phys. Oceanogr.*, *40*, 1539–1557, doi:10.1175/2010JPO4480.1.

Fyfe, J. C., O. A. Saenko, K. Zickfeld, M. Eby, and A. J. Weaver (2007), The role of poleward-intensifying winds on southern ocean warming, *J. Clim.*, *20*(21), 5391–5400, doi:10.1175/2007JCLI1764.1.

Gomez, N., J. X. Mitrovica, P. Huybers, and P. U. Clark (2010), Sea level as a stabilizing factor for marine-ice-sheet grounding lines, *Nat. Geosci.*, *3*(12), 850–853, doi:10.1038/ngeo1012.

Gregory, J. M., et al. (2013), Twentieth-century global-mean sea level rise: Is the whole greater than the sum of the parts? *J. Clim.*, *26*(13), 4476–4499, doi:10.1175/JCLI-D-12-00319.1.

Griffies, S. M., et al. (2009), Coordinated Ocean-ice Reference Experiments (COREs), *Ocean Modell.*, *26* (1-2), 1–46, doi:10.1016/j.ocemod.2008.08.007.

Griffies, S. M., and R. J. Greatbatch (2012), Physical processes that impact the evolution of global mean sea level in ocean climate models, *Ocean Modell.*, *51*, 37–72, doi:10.1016/j.ocemod.2012.04.003.

Landerer, F. W., J. H. Jungclaus, and J. Marotzke (2007), Regional dynamic and steric sea level change in response to the IPCC-A1B scenario, *J. Phys. Oceanogr.*, *37*, 296–312, doi:10.1175/JPO3013.1.

Large, W. G., and S. G. Yeager (2009), The global climatology of an interannually varying air-sea flux data set, *Clim. Dyn.*, *33*, 341–364, doi:10.1007/s00382-008-0441-3.

Lowe, J. A., and J. M. Gregory (2006), Understanding projections of sea level rise in a Hadley Centre coupled climate model, *J. Geophys. Res.*, *111*, C11014, doi:10.1029/2005JC003421.

McGregor, S., A. Sen Gupta, and M. H. England (2012), Constraining wind stress products with sea surface height observations and implications for pacific ocean sea level trend attribution, *J. Clim.*, *25*(23), 8164–8176, doi:10.1175/JCLI-D-12-00105.1.

Meijers, A. J. S., E. Shuckburgh, N. Bruneau, J.-B. Sallee, T. J. Bracegirdle, and Z. Wang (2012), Representation of the Antarctic Circumpolar Current in the CMIP5 climate models and future changes under warming scenarios, *J. Geophys. Res.*, *117*, C12008, doi:10.1029/2012JC008412.

Meredith, M. P., and A. M. Hogg (2006), Circumpolar response of Southern Ocean eddy activity to a change in the Southern Annular Mode, *Geophys. Res. Lett.*, *33*, L16608, doi:10.1029/2006GL026499.

Morrison, A. K., and A. M. Hogg (2013), On the relationship between southern ocean overturning and ACC transport, *J. Phys. Oceanogr.*, *43*(1), 140–148, doi:10.1175/JPO-D-12-057.1.

Sen Gupta, A., and M. H. England (2006), Coupled ocean–atmosphere–ice response to variations in the southern annular mode, *J. Clim.*, *19*(18), 4457–4486, doi:10.1175/JCLI3843.1.

Shakespeare, C. J., and A. M. Hogg (2012), An analytical model of the response of the meridional overturning circulation to changes in wind and buoyancy forcing, *J. Phys. Oceanogr.*, *42*(8), 1270–1287, doi:10.1175/JPO-D-11-0198.1.

Sijp, W. P., and M. H. England (2009), Southern Hemisphere westerly wind control over the ocean's thermohaline circulation, *J. Clim.*, *22*, 1277–1286, doi:10.1175/2008JCLI2310.1.

Slangen, A. B. A., C. A. Katsman, R. S. W. van de Wal, L. L. A. Vermeersen, and R. E. M. Riva (2012), Towards regional projections of twenty-first century sea-level change based on IPCC SRES scenarios, *Clim. Dyn.*, *38*(5-6), 1191–1209, doi:10.1007/s00382-011-1057-6.

Spence, P., J. C. Fyfe, A. Montenegro, and A. J. Weaver (2010), Southern ocean response to strengthening winds in an eddy-permitting global climate model, *J. Clim.*, *23*, 5332–5343, doi:10.1175/2010JCLI3098.1.

Thompson, D. W. J., S. Solomon, P. J. Kushner, M. H. England, K. M. Grise, and D. J. Karoly (2011), Signatures of the Antarctic ozone hole in Southern Hemisphere surface climate change, *Nat. Geosci.*, *4*(11), 741–749, doi:10.1038/ngeo1296.